POAC'13
Espoo, Finland

Proceedings of the 22nd International Conference on
Port and Ocean Engineering under Arctic Conditions
June 9-13, 2013
Espoo, Finland

THE CONSOLIDATION OF RAFTED SEA ICE: LABORATORY EXPERIMENTS AND MODEL VALIDATION

Eleanor Bailey [1], P. R. Sammonds [2,3], D. L. Feltham [3].
[1]Centre for Arctic Resource Development, C-CORE, St. John's, NL, A1B 3X5, Canada.
[2]Rock & Ice Physics Laboratory, Department of Earth Sciences, University College London, London, WC1E 6BT, United Kingdom.
[3]Centre for Polar Observation and Modelling, Department of Meteorology, University of Reading, Reading, RG6 6BB, United Kingdom.

ABSTRACT

A model for the consolidation of rafted sea ice has been developed that predicts how long it takes for the layers in a section of rafted sea ice to bond into a coherent ice sheet. The rafted ice is assumed to be composed of layers of sea ice of equal thickness, separated by thin layers of ocean water. Heat transport within the sea ice is described using the mushy layer equations and the rate of freezing is given by the Stefan condition. Concurrent laboratory experiments were conducted in the Rock and Ice Physics Laboratory at University College London (UCL). To simulate a section of rafted sea ice, blocks of laboratory-grown saline ice were stacked with 1 cm spacers between adjacent ice blocks to allow water to flood in. The consolidation process was monitored using temperature readings recorded in the ice and liquid layer, salinity measurements of the liquid layer and cores taken at specific times of interest. Results from the laboratory tests showed that the rafted ice had physically bonded in less than a day; however, it took many more days for the blocks to reach maximum strength. Comparison between numerical simulations and experiments showed that the model can predict when the ice sheets physically bond to within 10% accuracy. Further work is needed before the model can predict when the bond has reached maximum strength.

INTRODUCTION

Thick sea ice features such as ridges or rafted sea ice are a hazard to offshore operations, as when driven by wind or ocean currents, they have the potential to exert huge forces on drilling rigs or artificial islands. Ridges are elongated piles of rubble, and rafting is the overriding of one sheet by another. Two types of rafting have been observed. The first type is simple rafting, whereby the two ice sheets interact along a straight edge and one sheet overrides the other. The second type is finger rafting, whereby the interacting sheets fracture along lines perpendicular to their interacting edge and form fingers; alternate fingers are then over-thrust and under-thrust, leaving an interlocked structure (Weeks and Kovacs, 1970). Multiple rafting is also known to occur in some regions, where ice floes override one another multiple times to produce thick sea ice features (Babko et al., 2002). This process is particularly common in the north Caspian Sea where rafted sections of up to 13 layers have been observed, giving a total ice thickness of up to four meters (D. Mayne, personal communication, 2007).

An ice feature can represent a zone of either weakness or strength in the pack ice depending on the degree of consolidation (Hoyland, 2002). In a rafted section, the layers of sea ice are

initially separated by thin layers of ocean water. The bonds between the layers are at first weak but strengthen with time to produce a coherent, consolidated ice sheet. At present most design loads assume that the compressive strength of rafted ice is 10-20% less than that of level ice of the same thickness (Jizu et al., 1991). This is because it is believed that the bonds between layers in a rafted section may be weaker than solid ice. There is very little experimental or theoretical data to back this theory. The only systematic set of experiments were carried out by Poplin and Wang (1994), who measured the uniaxial compressive strength of rafted ice and compared it to corresponding landfast ice samples. Their results showed that, on ice samples cut horizontal to the crystal growth direction, the mean strengths of consolidated rafted ice at strain rates of 10^{-4} and 10^{-5} s^{-1} were actually higher than the landfast samples. They attributed these differences to variations in crystallographic structure. The landfast ice samples contained only columnar ice crystals, whereas the rafted ice was composed of approximately 50% granular ice and 50% mixed granular and columnar ice crystals. Since ice loads are usually applied horizontally to offshore structures, this result implies that once consolidated, rafted ice may be a significant ice hazard. Increased knowledge of the physical and mechanical properties of rafted sea ice is necessary to improve confidence in load estimates associated with this hazard.

Bailey et al. (2010) formulated a one-dimensional, thermal-consolidation model for rafted sea ice that predicts the time taken for layers of rafted sea ice to bond into a coherent ice sheet. At that time, there was no data with which to test the model. Bailey et al. (2012) later conducted a series of tests in the Ice Physics Laboratory at UCL to investigate the consolidation and strength of rafted sea ice. In this paper, the model is tested against this laboratory data and suggestions made for improving the model.

MODEL DESCRIPTION

Consider the situation where two identical ice sheets of initial thickness H_0 have rafted such that there is a liquid layer of initial thickness h_0 located between adjacent sheets (Figure 1). The sea ice is described as a mushy layer, a rigid matrix of pure ice immersed in its brine, and the liquid layer is a thin layer of ocean water, trapped between the asperities of the ice sheets. The internal temperature of each ice sheet is determined from the nonlinear one-dimensional heat diffusion equation,

$$c_{eff}\frac{\partial T}{\partial t} = \frac{\partial}{\partial z}\left(k_{eff}\frac{\partial T}{\partial z}\right), \qquad (1)$$

where c_{eff} and k_{eff} are, respectively, the effective volumetric specific heat capacity and the thermal conductivity of sea ice, T is the temperature within the ice sheet, t is time, and z is the vertical spatial coordinate (Feltham et al., 2006).

The sea ice initially has a linear temperature profile based on the air and sea temperature at the upper and lower boundaries, giving the following initial condition,

$$T = \frac{T_0 - T_L(S_{ocean})}{H_0}z + T_L(S_{ocean}) \qquad (\mathrm{t} = 0), \qquad (2)$$

where T_0 is the initial temperature at the upper surface, $T_L(S_{ocean})$ is the liquidus (freezing) temperature of the ocean at salinity S_{ocean} and H_0 is the initial thickness of the sea ice.

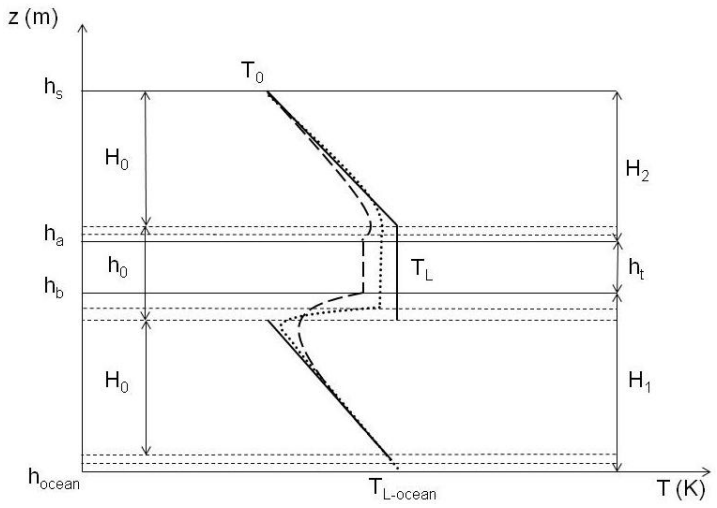

Figure 1. Schematic of the consolidation model illustrating how the temperature profiles, thickness of the ice sheets and the liquid layer evolve with time.

At the upper surface of the sea ice ($z = h_s$), it is assumed there is no melting so that the net flux, $(F_{net})_0$, is equal to the conductive flux, $-k_{eff}\,\partial T/\partial z$, such that

$$(F_{net})_0 \equiv \varepsilon_i(F_{LW} - \sigma T_0^4) + (1-\alpha)(1-I_0)F_{SW} - F_{sens} - F_{lat} = -k_{eff}\frac{\partial T}{\partial z} \qquad (z = h_s), \tag{3}$$

where ε_i is the emissivity of bare ice, F_{LW} is the flux of downward longwave radiation, σ is the Stefan-Boltzmann constant, I_0 is the fraction of incident radiation that passes through the surface into the interior of the ice, α is the albedo for bare ice, and F_{sens} and F_{lat} are the sensible and latent heat fluxes (Ebert and Curry, 1993).

At the interior interfaces ($z = h_a, h_b$), i.e. the interfaces above and below the liquid layer, the boundary conditions are

$$T = T_L(S_{liquid}) \qquad (z = h_a, h_b) \tag{4}$$

and

$$\mathcal{L}_s\phi\left(\frac{\rho_{brine}}{\rho_{ice}}\right)\frac{dh_{a,b}}{dt} = k_{eff}\frac{\partial T}{\partial z} \qquad (z = h_a, h_b), \tag{5}$$

where S_{liquid} is the salinity of the liquid layer, $\mathcal{L}_s$ is the volumetric heat of fusion of pure ice, $\phi = 1 - S_{bulk}/S_{liquid}$ is the local solid fraction per unit volume of the sea ice, $\rho_{brine}/\rho_{ice} = 1.09$ describes the expansion of the liquid upon freezing (Pounder, 1965), dh/dt is the velocity of the respective boundary and $\partial T/\partial z$ is the temperature gradient in the ice at the boundary.

At the sea ice–ocean boundary ($z = h_{ocean}$), the sea ice is held constant at the freezing temperature of the ocean,

$$\mathrm{T} = \mathrm{T_L}(\mathrm{S_{ocean}}) \qquad (z = h_{ocean}). \tag{6}$$

The ice growth rate at the ice–ocean boundary is given by the Stefan condition,

$$\mathcal{L}_s\phi\left(\frac{\rho_{brine}}{\rho_{ice}}\right)\frac{dh_{ocean}}{dt} = k_{eff}\frac{\partial T}{\partial z} + F_{ocean} \qquad (z = h_{ocean}), \tag{7}$$

where F_{ocean} is the heat flux from the ocean directed into the base of the ice sheet.

Since the liquid layer is narrow, the temperature within it is assumed to be uniform and equal to the local liquidus temperature, T_{liquid}, which can be approximated by the liquidus curve for sodium chloride (NaCl) solutions (Weast, 1971),

$$T_{liquid} = -5.33 \cdot 10^{-7} {S_{liquid}}^3 - 9.37 \cdot 10^{-6} {S_{liquid}}^2 - 0.0592 S_{liquid} + 273.15 \text{ K}. \quad (8)$$

The liquid layer is initially assumed to consist of ocean water and, as it freezes, a fraction of salt f originally contained in the sea water is released into the liquid layer. Therefore conservation of salt implies

$$S_{liquid} = S_{ocean} + f S_{ocean} \left(\frac{h_0}{h_t} - 1 \right), \quad (9)$$

where h_t is the thickness of the liquid layer at time *t*. The rate of change of h_t can be deduced from the difference in the Stefan conditions at the boundaries above and below the liquid layer, so that

$$\frac{dh_t}{dt} = \frac{k_{eff}}{\phi L} \frac{\rho_{ice}}{\rho_{brine}} \left(\frac{\partial T_a}{\partial z} - \frac{\partial T_b}{\partial z} \right), \quad (10)$$

where $\partial T_a / \partial z$, $\partial T_b / \partial z$ are the temperature gradients at the boundaries above ($z = h_a$) and below ($z = h_b$) the liquid layer respectively. The system of equations (Eqs. 1 to 10) comprises a closed partial-differential, initial-boundary value problem.

EXPERIMENTS

Method

A series of experiments were set up in the Ice Physics Laboratory at UCL to investigate the consolidation of rafted sea ice (Bailey et al. 2012). To set up an experiment, columnar grained blocks of ice were grown from a six parts per thousand (ppt) solution of NaCl to a thickness of 7 cm in a temperature-controlled cold room. This concentration and thickness was chosen to mimic conditions in the North Caspian Sea, where rafting is a predominant feature in thin ice. The tanks, acrylic cylinders 33 cm in diameter by 50 cm in length, were insulated with 20 cm thick tubes of polystyrene to ensure ice growth from the top down. At the base of each cylinder, a temperature controlled heater plate held the water below the growing ice block at its freezing temperature. Trace heating, embedded within the polystyrene insulation, eased the removal of the ice block. The blocks were sawn flat and stacked in the tank with 1 cm spacers between the ice blocks. Once assembled, the ice blocks were then left to consolidate in a room held at a nominal temperature of -10±1°C. Figure 2 shows a schematic of the experimental set up.

Temperature was measured at the ice–atmosphere surface, in the ice blocks and in the liquid layer, using custom-built thermistor probes (accuracy of ±0.4°C). The salinity of the liquid layer was measured by taking samples through a hole drilled into the side of the acrylic cylinder and sealed with a re-sealable bung. Samples were extracted from the liquid layer using a hypodermic needle and syringe, and the salinity measured using a MISCO digital refractometer (accurate to ±0.5 ppt). The temperature and salinity measurements were then

used, along with ice cores taken from the rafted ice blocks at particular times of interest, to determine the rate of consolidation.

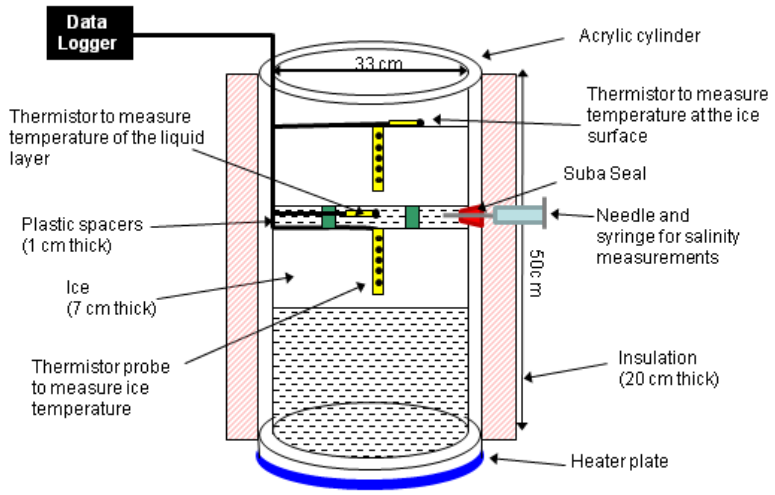

Figure 2. Schematic diagram showing the experimental set-up for the rafted ice consolidation experiments.

Results

Figure 3 shows the temperature recorded in the ice blocks and the liquid layer as a function of depth and time. The dotted line shows the temperature in the ice blocks prior to the trace heating being turned on, and the solid lines the temperature profiles at different times during consolidation. In the first 5 minutes of consolidation, the temperature in the upper block rose by ~1°C, which is a consequence of the trace heating. After ~250 minutes, the temperature in the upper block had re-established a linear temperature profile, and in the lower ice block the temperature had increased to a constant temperature of -0.8°C. After this, both ice blocks continued to cool until the experiment was stopped after 25900 minutes (17 days, 23 hrs, 40 mins). An almost-linear temperature profile was achieved throughout both ice blocks and the liquid layer after ~1300 minutes. This time coincides with the time that ice growth was observed to start at the base of the rafted section.

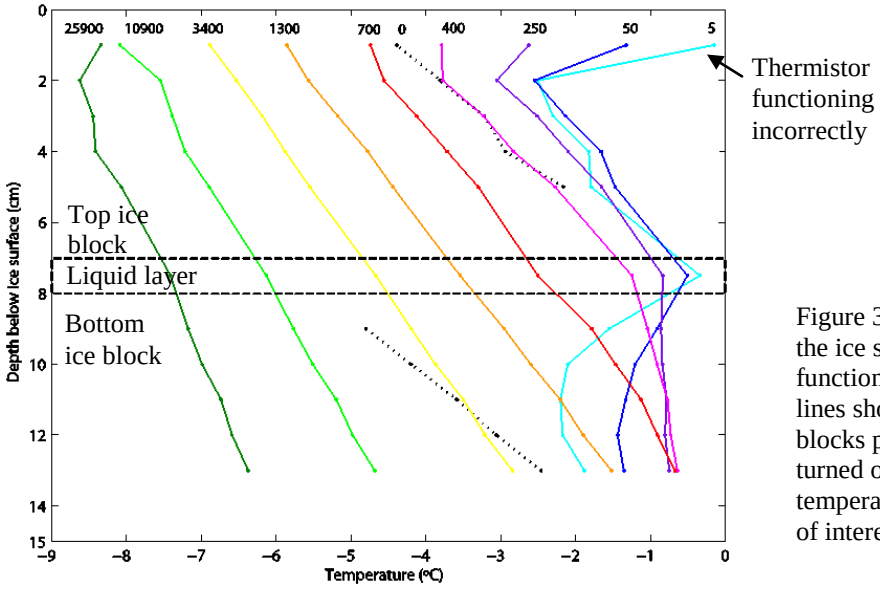

Figure 3. The temperature evolution in the ice sheets and the liquid layer as a function of depth and time. The dotted lines show the temperature in the ice blocks prior to the trace heating being turned on, and the solid lines the temperature profiles at different times of interest.

Figure 4 shows the temperature evolution of the liquid layer between the two rafted ice blocks, recorded by a single thermistor probe sandwiched between the two ice blocks. The figure shows that there is a plateau in the first ~250 minutes during which there is little change in temperature and after which the temperature decreases rapidly from -0.8°C to -3°C. The temperature trace then gradually flattens with time, until the end of the experiment, reaching a final temperature of -7.4°C. It is interesting to note that after the rapid decrease in temperature, the small-scale fluctuations in the temperature traces become more prominent, perhaps indicating that the liquid layer has frozen. (The small fluctuations in temperature result from the cold room defrost cycle, which caused the ice to warm by less than 0.25°C). It is difficult to pinpoint an exact time that this change in behaviour takes place as it is a gradual process occurring over several hundred minutes. By enlarging the plot and fitting a best fit line, rapid cooling can be estimated to cease after ~700 minutes.

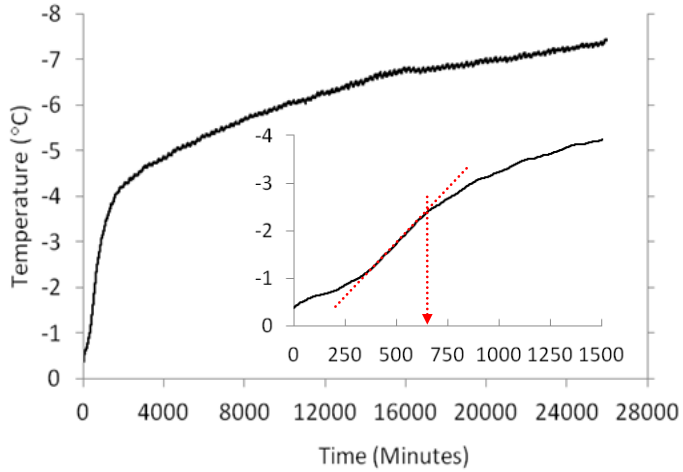

Figure 4. Temperature evolution of the liquid layer recorded by a single thermistor probe located between the two ice blocks. The enlarged plot shows a zoom of the first 1500 minutes of consolidation. The best fit-line superimposed on the plot shows that the temperature starts to deviate from a rapid temperature decrease to a more gradual trend after ~700 minutes.

In addition to measuring the temperature in the liquid layer, its salinity was also measured by taking samples with the needle and syringe. These values are plotted against time in Figure 5. Also included in this plot are salinity measurements that were estimated using the inverted liquidus curve (Eq. 8) and the temperature readings recorded in the liquid layer. The fact that the inverted temperature readings are in good agreement with the measured samples demonstrates that the assumption made in the model that the liquid layer is held at its freezing temperature is reasonable. The figure shows that similar to the temperature in the liquid layer, in the first ~250 minutes the salinity of the liquid layer increased only fractionally. The salinity then increased rapidly from ~14 ppt to 50 ppt and then gradually levelled out reaching a final salinity of 100 ppt by the end of the experiment. Constant salinity was taken as an indicator that the experiment could be terminated, which was done after a further two days.

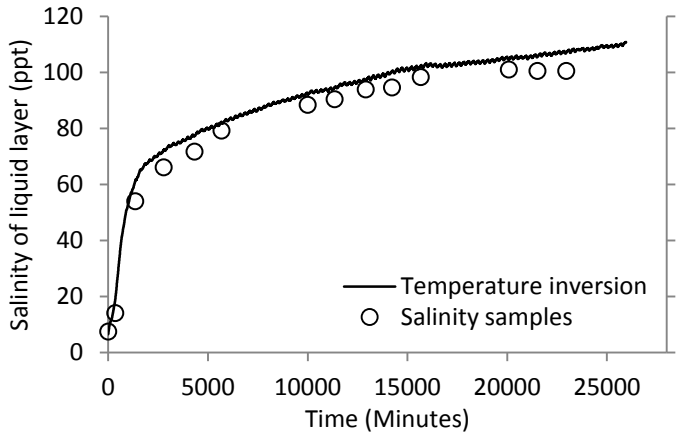

Figure 5. Salinity evolution in the liquid layer during the standard case experiment. The circles represent the samples that were taken with a needle and syringe and the solid line the temperature readings that were inverted using the liquidus curve (Eq. 8).

To determine when the ice blocks had consolidated, the experiment was repeated six times taking cores at different times of interest. In Table 1, the times at which cores were taken with the observed states of consolidation are presented. At 460 minutes, the ice was not sufficiently bonded to allow one to core through both ice blocks and the lower ice block was pushed away by the corer. At 770 minutes, it was possible to take a core of both ice blocks, but the bond was so weak that the core fell apart; when viewing the remaining ice in the tank it was clear that the ice blocks had physically bonded and there was no liquid layer present. This coincides with the time that the temperature in the liquid layer stopped decreasing rapidly (Figure 4). By 1610 minutes, the ice had sufficiently bonded to take an intact core; however, a weak layer could still be felt on coring. By 11300 minutes, resistance to coring was consistent, indicating that there is no weak layer present.

Table 1. Times that cores were taken of the standard case rafted ice experiment

Time core taken (Minutes)	Time core taken (Hours)	Consolidated (Yes/No)	Experimental Notes
460	7hrs, 40mins	No	Could only core through upper ice block - lower ice block pushed away with pressure of coring
770	12 hrs, 50mins	Yes	No liquid layer present – very weak bond core broke in two
1110	18hrs, 30mins	Yes	No liquid layer present – very weak bond core broke in two
1610	1day, 2hrs, 50mins	Yes	Felt a weak layer when coring
7250	5days, 50mins	Yes	Felt strong when coring
11,300	7days, 20hrs	Yes	Felt very strong when coring – no obvious weak layer

TESTING THE RAFTED ICE CONSOLIDATION MODEL

The rafted ice consolidation model was tested against laboratory data using input parameters consistent with those used in the experiments described above. It was not possible to estimate the atmospheric and oceanic heat fluxes during the experiment; therefore, the boundary condition at the ice–atmosphere interface (Eq. 3) and the Stefan condition at the ice–ocean interface (Eq. 7) were constrained by using the temperature measured at the ice–atmosphere surface and the growth rate measured during the laboratory experiments.

Test 1

In the first test, the temperature of the liquid layer was constrained using values derived from experiments so that the uncertainty in the brine release process could be ignored while other processes were investigated. This means that equations (8) and (9) no longer need to be solved and the temperature of the liquid layer can simply be updated at every time step.

The results from this simulation showed that the ice sheets did not consolidate and that the thickness of the liquid layer started to increase after ~350 minutes. This is because, as Figure 6 shows, the position of the freezing front located below the liquid layer (h_b) started to melt after ~250 minutes, causing the liquid layer to migrate downwards. The ice melts because the temperature of the liquid layer, being at the liquidus temperature appropriate to its high salinity, is lower than the temperature in the lower ice sheet. This promotes a negative temperature gradient in the lower ice block, causing sensible heat to be extracted from the lower block and converted into the latent heat of the liquid phase. Because the liquid layer is

assumed to have a constant temperature, heat cannot diffuse in the liquid layer and therefore causes melting at h_b.

It is clear from the experiments that the ice sheets did in fact consolidate; therefore, it is believed that this migration of the liquid layer is an artefact of the model. To solve this problem, in Test 2 the model was constrained so that no melting could take place at h_b.

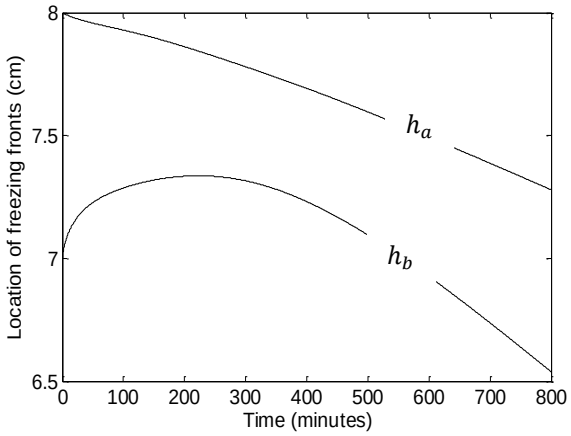

Figure 6. The location of the freezing interfaces above (h_a) and below (h_b) the liquid layer as a function of time for Test 1.

Test 2

In this test, the model was constrained by adding a line of code which imposed the condition that when the growth rate of the ice sheet below the liquid layer is less than zero (i.e. $dh_b/dt < 0$), $dh_b/dt = 0$, so that that no melting can take place and h_b remains at the same position. The effect of this can be seen clearly in Figure 7, which shows the location of the freezing fronts for this test. The figure shows that initially ice growth is predominantly at h_b, as heat was conducted from the liquid layer into the lower ice block. After ~200 minutes, ice growth ceased at h_b and the position of the interface remained constant. Ice growth then only took place at h_a and continued until the liquid layer completely froze, after 750 minutes. This is similar to the time at which the ice blocks had physically bonded in the experiments.

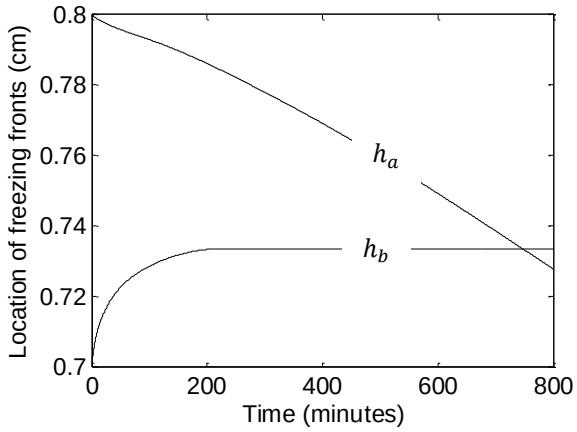

Figure 7. The location of the freezing interfaces above (h_a) and below (h_b) the liquid layer as a function of time for Test 2.

Figure 8 shows the temperature profiles predicted by the model and the values recorded by the thermistors in the experiment. The figure shows that the two sets of data are in very good agreement, demonstrating that the mushy layer equations can accurately predict the temperature distribution in the ice.

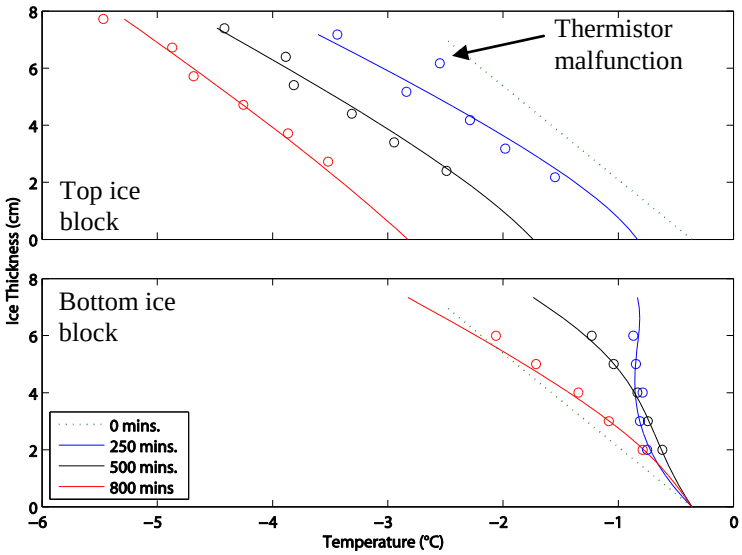

Figure 8. The temperature evolution in the ice blocks for Test 2. The values predicted by the model are shown by the solid lines and those recorded by the thermistors in the experiments are shown by the circles.

Test 3

In the third test, the temperature of the liquid layer was no longer constrained using experimental data, so that the brine release process could be investigated. Since the fraction of salt released into the liquid layer (f) is uncertain (Eq. 9), the model was run for a number of different values of f.

In Figure 9, the positions of the freezing fronts for the different values of f are presented. The figure shows that the greater the value of f, the slower the rate of freezing. This is as expected, since the more salt expelled into the liquid layer, the more heat that needs to be extracted for subsequent freezing to take place. For comparison, the results from Test 2 (bold dashed line), where the temperature of the liquid layer was constrained using data measured in the experiments, are also plotted. The rate of freezing at h_b in Test 2 is almost exactly the same as that found in the simulation run with $f = 60\%$. However, at h_a the growth rate found in Test 2 varies between those found in the 60% and 100% simulations. This suggests that the value of f lies in the range of 60 – 100%.

From Figure 9, it is evident that in the simulations the liquid layer will never completely freeze over (unless it reaches the eutectic temperature). This is because as long as a fraction of salt is released into the liquid layer there will always be a liquid layer remaining, even if it is infinitely thin. The model assumes that the surfaces of the ice slabs are smooth, whereas in reality they are rough. At some stage the surface asperities will grow sufficiently in size to effectively bond the slabs together. We therefore imposed a 'cut-off' in the code such that when the liquid layer reaches the size of the surface asperities (h_{sa}) the adjacent ice sheets can be considered consolidated. From conservation of salt, h_{sa} can be estimated from

$$h_{sa} = \frac{h_0}{\frac{S_t - S_{ocean}}{f S_{ocean}} + 1}, \qquad (11)$$

where $S_t = 42$ ppt is the concentration of the liquid layer immediately prior to consolidation (taken from Figure 5).

The simulations run with f =10, 30, 60 and 100%, correspond respectively to surface asperity heights of 0.21, 0.6, 1.15 and 1.79 mm. Employing these cut-offs reveal that the liquid layer consolidated at 599, 634, 649 and 653 minutes respectively. These consolidation times predicted by the model are again similar to the times that the ice blocks had physically bonded in the experiments.

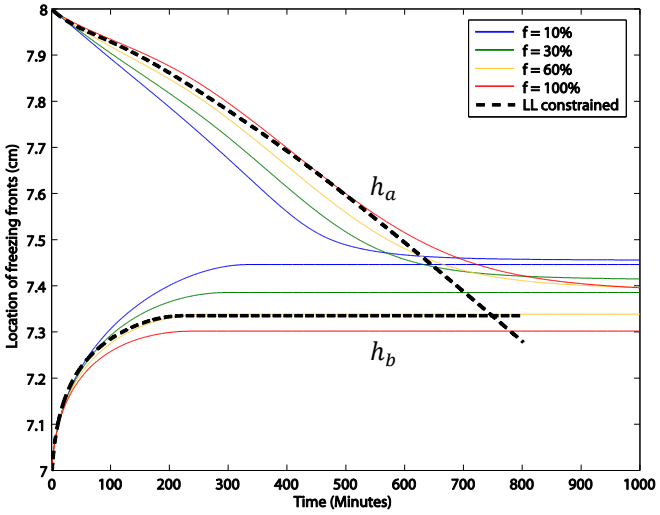

Figure 9. The location of the freezing interfaces above (h_a) and below (h_b) the liquid layer for Test 3, where the fraction of salt release (f) was set to 10 (blue line), 30 (green line), 60 (orange line) and 100 % (red line). Also included in this plot are the values obtained when the temperature of the liquid layer (LL) was constrained (i.e. Test 2).

DISCUSSION AND CONCLUSIONS

In this paper, a rafted ice consolidation model is presented that calculates the time taken for two layers of ice to bond effectively into a coherent ice sheet. The model was then tested against experimental data that was collected during a series of tests conducted in the Ice Physics Laboratory at UCL.

Results from laboratory experiments showed that the salinity of the liquid layer increased over the course of the experiment. As the liquid layer freezes, increasing amounts of salt are released into the remaining liquid layer. This in turn causes a reduction in the temperature of the liquid layer as it cools to its freezing temperature. The salinities obtained by inverting the temperature using the liquidus curve are in good agreement with the direct salinity measurements, demonstrating that the assumption made in the model, that the liquid layer is held at its freezing temperature, is reasonable. The temperature in the liquid layer decreased rapidly at first and continued until the rafted ice was physically bonded (which was confirmed by taking cores at specific times of interest). At this point the bond was still physically weak because the consolidated liquid layer had a high liquid fraction. The strength of the bond then gradually increased as the temperature and the liquid fraction decreased.

Comparison of results from laboratory experiments and model tests showed some notable differences. Most importantly, the consolidation model predicts that the liquid layer would not freeze and would migrate downwards. This was clearly not the case experimentally. The variance owes to the assumption that the liquid layer has a spatially uniform temperature and salinity, which only holds if the liquid layer is sufficiently narrow that diffusion homogenises the salt distribution within the layer. Feltham (1998) showed that for this condition to be satisfied $(h/H)^2 \ll Le$, where h is the gap thickness, H is the thickness of the ice sheets and $Le \approx 10^{-2}$ is the Lewis number, defined to be the diffusion rate of salt divided by the effective thermal diffusivity of sea ice. In the laboratory experiments the gap thickness was 1

cm and the ice sheets were 7 cm thick, resulting in $(h/H)^2 \simeq 0.02$. This implies that the salt may not be evenly distributed across the liquid layer.

In order to compensate for this, the model was constrained so that no melting can take place at the top of the lower ice block, thereby preventing the liquid layer from migrating downwards. This constraint significantly improved the predictions of the model, finding consolidation times that were similar to those found in the experiments. To investigate what fraction of salt f was released into the liquid layer, the model was run for a range of values and results compared with the experiments. Results showed that the simulations run with f ranging between 60% and 100% gave the best results.

The model as it stands can only predict when the ice sheets will physically bond, and not when they reach their maximum strength. The latter is certainly of more interest to engineers when calculating loads for offshore structures. Predicting the time at which ice sheets will have reached their maximum strength could be quite straightforward; for example, it could be done by merging the ice sheets and the consolidated liquid layer into a single ice block and running the simulation until the solid fraction in the liquid layer becomes constant. The model could also be improved by modelling the temperature and salinity distributions in the liquid layer and accounting for brine drainage into and/or out of the liquid layer.

REFERENCES

Babko, O., D.A. Rothrock, and Maykut, G.A., 2002. Role of rafting in the mechanical redistribution of sea ice thickness, J. Geophys. Res., 107(C8), 3113, doi:10.1029/1999JC 000190.

Bailey, E., Feltham, D.L. and Sammonds, P.R., 2010. A model for the consolidation of rafted sea ice, J. Geophys. Res., Vol. 115 (C04015), doi:10.1029/2008JC005103.

Bailey, E., Sammonds, P.R. and Feltham, D.L., 2012. The consolidation and bond strength of rafted sea ice, Cold Reg. Sci. and Technol., Vol. 83-84, pp. 37-48, ISSN 0165-232X, doi:10.1016/j.coldregions.2012.06.002.

Ebert, E., and Curry, J. A., 1993. An intermediate one-dimensional thermodynamic sea ice model for investigating ice-atmosphere interactions, J. Geophys. Res., 98, 10085-10109.

Feltham, D.L., 1998. Fluid dynamics and thermodynamics of sea ice, Ph.D. thesis, University of Cambridge, Cambridge, U.K.

Feltham, D.L., Untersteiner, N., Wettlaufer, J.S. and Worster, M.G., 2006. Sea ice is a mushy layer, Geophys. Res. Lett., 33, L14501, doi:10.1029/2006GL026290.

Hoyland, K.V., 2002. Consolidation of first-year sea ice ridges, J. Geophys. Res., 107(C6), 3062, doi:10.1029/2000JC000526.

Jizu, X., Qingzeng, S., An, S., Yunlin, F., and Tongkui, L., 1991. Sea Ice Engineering in China, Journal of Coastal Research, 7(3), 759-770.

Poplin, J.P., and Wang, A.T., 1994. Mechanical properties of rafted annual sea ice, Cold Reg. Sci. Technol., 23, 41-67.

Pounder, E.R., 1965, The Physics of Ice, Pergamon Press, Oxford.

Weast, R.C., 1971. Handbook of chemistry and physics, Fifty-second ed., Cleveland, OH, Chemical Rubber Co.

Weeks, W.F., and Kovacs, A., 1970. On pressure ridges, CRREL Rep. IR505, U.S. Army Cold Regions Res. and Eng. Lab., Hanover, N. H.